A Mechanochromic Rotaxane that Releases Azetidine-Trityl- Maleimide, a Versatile Fluorescent Probe

DOI:
10.1002/anie.202501499

Document Version
Accepted author manuscript

A Journal of the Gesellschaft Deutscher Chemiker

Angewandte International Edition GDCh Chemie

www.angewandte.org

Accepted Article

Title: A Mechanochromic Rotaxane that Releases Azetidine-Trityl-Maleimide, a Versatile Fluorescent Probe

Authors: Mengjiao Wu and Guillaume De Bo

To be cited as: *Angew. Chem. Int. Ed.* **2025**, e202501499

Link to VoR: https://doi.org/10.1002/anie.202501499

WILEY VCH

10.1002/anie.202501499

WILEY VCH

COMMUNICATION

A Mechanochromic Rotaxane that Releases Azetidine-Trityl-Maleimide, a Versatile Fluorescent Probe

Mengjiao Wu,[a] and Guillaume De Bo*[a]

[a] Dr. M. Wu, Prof. Dr. G. De Bo
Department of Chemistry, University of Manchester, Oxford Road, Manchester M13 9PL, United Kingdom
E-mail: guillaume.debo@manchester.ac.uk

Abstract: Force sensing at the molecular level has enabled the study of materials failure and it offers great promises for the investigation of mechanobiological processes. Traditional force probes rely on the reversible or irreversible activation of mechanochromic precursors to assess transient or permanent changes in the polymer networks. A promising approach involves force-controlled release of sensing molecules, as the accumulation of chromic molecules at specific sites would enable the recording of deformation histories. However, many fluorescent probes are limited by environmental sensitivity, specific release conditions, or low release efficiency. Maleimide-based dyes, especially amino maleimides, offer a robust alternative due to their small size, structural versatility, and tuneable fluorescence properties. Here, we present a mechanochromic rotaxane device that releases an azetidine-trityl-maleimide (ATM) fluorescent probe via a retro-[4+2] cycloaddition reaction. ATM, is a rigidochromic, chemically stable, and environmentally insensitive probe, generated exclusively through rotaxane actuation, underscoring the unique mechanochemical properties of rotaxanes. This device holds potential for applications in material science and biology, such as the investigation of polymer networks and active tissues.

The sensing of mechanical force at the molecular level has been instrumental in the investigation of mechanochemical processes involved in stress distribution, chain scission, and crack propagation in polymer materials.[1] These force probes usually rely on the reversible (cyclic[2] or interlocked[3]) or irreversible (scissile[4,5]) activation of a mechanochromic precursor. Though a reversible response proves useful to monitor transient deformations, an irreversible activation allows for the history of such deformation to be recorded (as the chromic molecules accumulate over multiple activation cycles).[6] In this context, the force-controlled release of sensing molecules[7] is particularly attractive as it would enable the accumulation of such probes at specific site (potentially with a better spatial resolution), and it offers the additional advantage of maintaining the integrity of the polymer architecture (i.e. the polymer doesn't break upon mechanophore activation) if such a release is operated from flex-activated,[7c] cyclic[8] or interlocked[9] mechanophores. However, the reading of this history depends on the stability of the probe itself, and many fluorescent probes show sensitivity to environmental conditions (polarity, pH, oxygen, moisture, nucleophiles…),[10] require specific release conditions (polarity, pH),[7a,b] or suffer from low release efficiency,[7c] which hampers their wider use in a material or biological context.

Maleimide-based dyes offer a great alternative, as they are small, structurally versatile, and possess highly tuneable fluorescence properties.[11] In fact, some have been used as fluorophores in scissile mechanophores.[5] Amino maleimides are highly emissive fluorophores endowed with large Stokes shifts and high quantum yields.[12] Amongst these, amino-trityl-maleimide derivatives present an interesting rigidochromic behaviour as the restricted rotation of the trityl group favours a radiative decay, which leads to a fluorescent emission with high quantum yield in rigid environments (e.g. solid state, viscous liquids).[13] However, their emission is sensitive to the polarity of these environments, partly due to the ability of the amino group to form hydrogen bonds.[14] Conveniently, their bulky size makes them suitable to be released by a rotaxane actuator. Indeed, we have recently demonstrated the use of such rotaxane actuator for the efficient force-controlled release of maleimide cargo molecules dispersed along its axle.[9]

Here, we describe a mechanochromic rotaxane device that releases an azetidine-trityl-maleimide (ATM) fluorescent probe (**2**, Figure 1b), as the pulling of the macrocycle against the bulky furan/maleimide Diels–Alder (DA) adduct leads to the irreversible release of ATM via a retro-[4+2] cycloaddition (Figure 1a-b). ATM is akin to a 'universal' probe as its fluorescence emission shows little dependence on environmental factors, such as polarity or pH, and it displays an excellent chemical stability. Moreover, the presence of a cyclic amine removes the H-bond donating ability, improving its fluorescence in solution. Remarkably, the mechanochemical generation of ATM is only possible within the confine of a rotaxane as the activation of the non-interlocked DA adduct leads to the separation of the trityl group from the maleimide precursor, further demonstrating the unique ability of rotaxanes to trigger mechanochemical transformations.[15] We anticipate that this mechanochromic rotaxane device will find application in materials and biology, for example for the investigation of the mechanics of polymer networks[16] and of active tissues.[17]

Our design is based on our previously reported cargo-releasing molecular device.[9] Rotaxane device $\mathbf{1}_{cis}$ is composed of a rotaxane actuator part, built around a pillar[5]arene (P5) macrocycle threaded onto a C12 alkyl chain, and a cargo compartment containing the DA adduct that releases the fluorescent azetidine maleimide cargo upon mechanical activation (Figure 1b). Elongation of $\mathbf{1}_{cis}$ triggers the pulling of the macrocycle along the axle until it meets the DA adduct, a steric obstacle for the small cavity of P5. The forceful contact between the macrocycle and the DA adduct eventually promotes the retro-

10.1002/anie.202501499

[4+2] cycloaddition that releases ATM and allows the macrocycle to escape the axle. This force-promoted reaction occurs via a pushing activation unique to the rotaxane architecture (Figure 1a).[18] The azetidine maleimide was selected for its photophysical properties and its ability to form stable DA adducts with furan derivative. Indeed, maleimides are small and versatile fluorescent probes, whose photophysical properties can be tuned by varying the substituents on the olefinic and/or nitrogen parts of the molecule.[11] Trityl maleimides present the double advantage of displaying rigidochromic properties and a large size, which makes them suitable to be released with our rotaxane actuator.[13] The presence of an electron donating azetidine ring shifts the absorption/emission of the molecule to a useful range (Figure 1a), and also suppresses the maleimide reactivity toward nucleophiles, enhancing its chemical stability. We tested several cyclic amines (piperidine, pyrrolidine, and azetidine), but only the azetidine substitution provided stable DA adducts (Scheme S4, Figures S1-S4).

In fact, the electron-donating nature of azetidine ring prevents the formation of a DA adduct by reacting **2** with furan derivative **6** (further demonstrating the excellent chemical stability of this probe). The desired adducts were obtained from the corresponding bromo adduct **7**, which was formed exclusively as the *exo* adducts after reacting furan **6** with bromo maleimide **5**. Both *cis* and *trans* adducts were formed (relating to the relative orientation of the Br atom and the alkynyl group in the adduct). Surprisingly, reacting one of these isomers (**7**$_{cis}$, shown in Figure 1c) with azetidine leads to a mixture of *cis* and *trans* azetidine substitution DA adducts, both as *endo* isomers. The stereochemistry was confirmed by the crystal structure of the *cis* adduct (**8**$_{cis}$, Figure 1c, SI Section 13).[19] This outcome suggests that the formation of **8**$_{cis/trans}$ proceeds via an elimination/addition sequence. Extension of rotaxane **11** with **9**$_{cis}$ delivers rotaxane **1**$_{R\text{-}cis}$, which can then be transformed into polymer **1**$_{P\text{-}cis}$ by single electron transfer living radical polymerization (SET-LRP),[20] or further modified to form a crosslinked network (see below). Polymer **1**$_{P\text{-}trans}$ was synthesised from **8**$_{trans}$ following the same route (see SI).

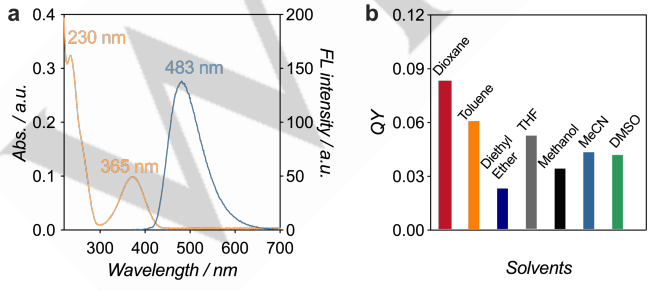

Figure 2. (a) The absorption and emission (λ_{ex} = 365 nm) spectra of molecule **2** in MeCN (c = 2 × 10^{-5} M). (b) Solution quantum yields (QY) for molecule **2** in different solvents.

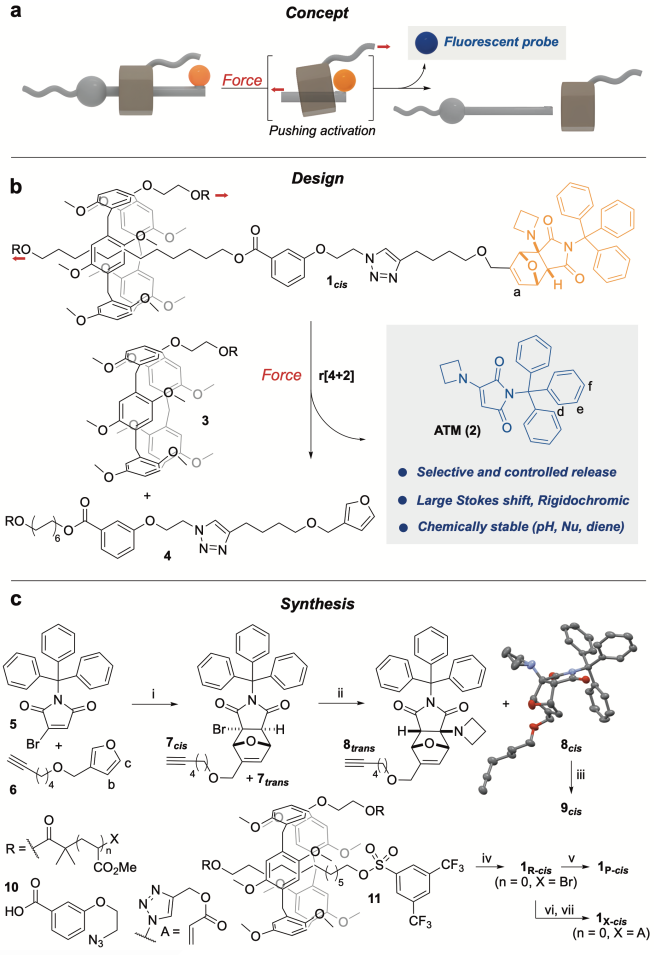

Figure 1. Mechanochemical release of ATM fluorescence probe. (a) Concept and (b) design of mechanochromic rotaxane **1**$_{cis}$ that releases ATM **2**. Red arrows indicate the direction of the force. (c) Synthetic route to linear PMA **1**$_{P\text{-}cis}$ and crosslinker **1**$_{X\text{-}cis}$. Conditions: (i) DMF, 70 °C, 12 h, 33% yield for **7**$_{cis}$, 27% yield for **7**$_{trans}$. (ii) Azetidine, K_2CO_3, MeCN, 0 °C - r.t., 12 h, 36% yield for **8**$_{cis}$, 36% yield for **8**$_{trans}$. Solid-state structure (XRD) of intermediate **8**$_{cis}$ shown (thermal ellipsoids at 50% probability, hydrogen atoms omitted for clarity). (iii) **10**, PMDETA, CuBr, DCM, r.t., 12 h, 50%. (iv) **9**$_{cis}$, K_2CO_3, 18-crown-6, acetone, r.t., 16 h, 59%. (v) Methyl acrylate, $CuBr_2$/Cu(0), Me_6TREN, DMSO, r.t., 2 h. (vi) NaN_3, DMSO, r.t., 2 h, 90%. (vii) Prop-2-yn-1-yl acrylate, PMDETA, CuBr, DCM, r.t., 12 h, 43%.

We first tested the UV-vis absorption and fluorescence emission of the ATM probe and found that it exhibited a large Stokes shift (118 nm) and an emission wavelength peaking at 483 nm (Figure 2a). ATM demonstrates a relatively constant fluorescence emission intensity across solvents of varying polarities (Figure 2b, SI Section 6.1). This contrasts with amino-trityl-maleimides built from primary amines as the H-bond donating ability of these maleimides provides a mechanism for fluorescence quenching.[14] ATM's rigidochromic behaviour was confirmed by the enhanced fluorescence quantum yield (QY = 46%) observed in the solid state (SI Section 6.1).[13] The ATM probe also displays excellent chemical stability; its fluorescence emission is stable under acidic (up to 100 mM TFA in MeCN) and basic (up to 500 mM Et_3N in MeCN) conditions (Figures S6-S7).

10.1002/anie.202501499

It is also inert to 1-dodecanethiol (Figure S8), an excellent nucleophile which usually react readily with maleimides, and to cycloaddition with dienes (see above).

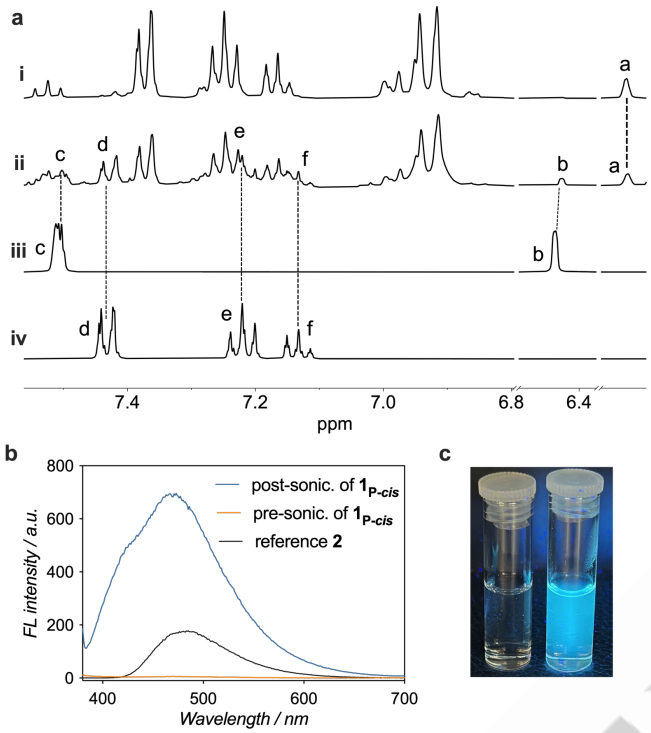

Figure 3. Sonication of polymer $\mathbf{1}_{P\text{-}cis}$ in MeCN. (a) Partial ^{1}H NMR (400 MHz, Acetone-d_6, 298 K) spectra comparison (i) polymer $\mathbf{1}_{P\text{-}cis}$, (ii) polymer $\mathbf{1}_{P\text{-}cis}$ after 150 minutes of sonication, (iii) reference molecule **6**, (iv) reference molecule **2**. (b) Fluorescence spectra (λ_{ex} = 365 nm) of polymer $\mathbf{1}_{P\text{-}cis}$ in MeCN before sonication, polymer $\mathbf{1}_{P\text{-}cis}$ in MeCN after 150 minutes of sonication (the shoulder peaking ~420 nm is due to the sonochemical degradation of MeCN solution, see Figure S16), reference molecule **2** in MeCN (c = 2 × 10^{-5} M). (c) Aliquots of the reaction mixture under 365 nm UV light before (left) and after (right) sonication showing the change in fluorescence.

Mechanical activation was performed in MeCN (20 kHz, 13.0 W/cm^2, 1s ON/ 1s OFF, 0-5 ˚C, 150 min) using high-intensity ultrasound (Figure 3, SI Section 7). The reaction was monitored by SEC and the sonication was stopped when the molecular weight was reduced by half. A comparison of the ^{1}H NMR spectra before and after sonication confirmed that the retro-Diels–Alder reaction occurred, driven by the rotaxane actuator (Figure 3a). Specifically, the post-sonication spectrum (ii, Figure 3a) showed the appearance of the characteristic peaks of furan (H_b, H_c) and azetidine maleimide (H_d, H_e, H_f), along with a reduction in the integration of the adduct (H_a). The mechanophore activation occurs exclusively via a r[4+2] pathway as no products arising from the cleavage of the C-N bond could be observed (Figures S9, S10). The mechanochemical nature of the activation was confirmed with control polymers (Figures S11, S12).

The release of the ATM probe was confirmed visually, by placing the sample under 365 nm light (Figure 3c), and spectroscopically, as the fluorescence spectra of the post-sonication mixture matches the emission of an independently synthesised ATM reference (Figure 3b). The release efficiency was also quantified from the relative integration of peaks H_a and H_b in the post-sonication ^{1}H NMR spectra (Figure 3a and Figures S9, S10, S13-S15, SI Section 7). Interestingly, polymers $\mathbf{1}_{P\text{-}cis}$ and $\mathbf{1}_{P\text{-}trans}$, which differ only by the orientation of the cargo-bearing DA adduct, show a significant difference in release efficiency (a difference not observed upon thermal activation, see SI Section 8), with $\mathbf{1}_{P\text{-}cis}$ releasing a larger amount of cargo and at a faster rate (Table 1), averaging 30% cargo release (unselective scission in the PMA backbone accounts for the difference).

Table 1. Structural and Activation Parameters.

Polymer	Pre-sonic. M_n (kDa) / $Đ$	Post-sonic. M_n (kDa) / $Đ$	r[4+2][a] (%)	Rate constant[b] (min^{-1}·kDa^{-1}·10^6)	F_{max}[c] (nN)
$\mathbf{1}_{P\text{-}cis}$	100 / 1.17	50 / 1.26	30	10.9	3.40
$\mathbf{1}_{P\text{-}trans}$	99 / 1.19	49 / 1.33	18	8.0	4.34

[a] Determined from the integration of furan and adduct olefinic peaks (e.g. *a*, *b* in the post-sonication ^{1}H NMR spectrum of $\mathbf{1}_{P\text{-}cis}$ (Figures 2a, S9)). [b] Determined from the slope of the linear fit in Figures S13c, S14c. See SI Section 7 for details. [c] Determined from CoGEF calculations. See SI Section 10 for details.

The observed difference in reactivity was reflected in the F_{max} values obtained from CoGEF (Constrained Geometries simulate External Force)[21] calculations (DFT B3LYP/6-31G*, vac.), as $\mathbf{1}_{P\text{-}cis}$ is predicted to break at a lower force than $\mathbf{1}_{P\text{-}trans}$ (Table 1 and SI Section 10). This can be explained by the fact that the azetidine ring is the first blocking group in the path of the macrocycle (i.e. the macrocycle pushes on the azetidine rather than directly on the trityl, see SI Section 10). Consequently, the pushing of the macrocycle against the azetidine ring in the *cis* isomer predominantly activates bond *a* located along the shortest path separating the blocking group from the axle of the rotaxane (unzipping geometry, Figure 4). In the *trans* isomer, the azetidine group is antipodal to the axle and the tension spreads equally over the cyclic system, producing a similar coupling at bond *a* and *b* (shearing geometry). Both isomers are predicted to break in a formal retro-[4+2] cycloaddition pathway (see SI Section 10). Remarkably, $\mathbf{1}_{cis}$ is the most reactive maleimide-based DA mechanophore described to date.[22] In contrast, the non-interlocked adduct, pulled from the trityl and the furan respectively, is predicted to break at the C-N bond connecting the maleimide to the trityl group (see SI Section 10). These results further highlight the importance of geometry in the activation of mechanophores,[23] and the unique ability of a rotaxane actuator to elicit reactivities inaccessible to the pulling actuation.[18]

10.1002/anie.202501499

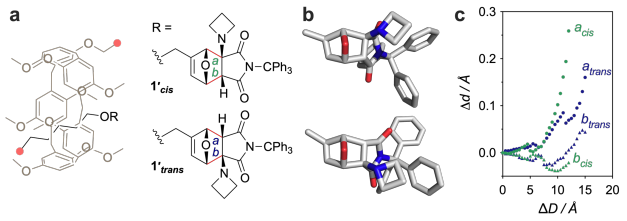

Figure 4. Computational investigation of the mechanochemical activation of *cis* and *trans* isomers of the DA adducts with a rotaxane actuator. (a) Rotaxane models **1′*cis*** and **1′*trans*** used in the computation indicating key structural parameters. Predicted scissile bonds are shown in red. Anchor atoms are indicated by pink disks. (b) Equilibrium geometries at E_{max} of the *cis* and *trans* Diels–Alder adduct mechanophores. Macrocycle and axle omitted for clarity. (c) Evolution of bond *a* and *b* upon simulated elongation of rotaxane **1′*cis*** (green) and **1′*trans*** (blue).

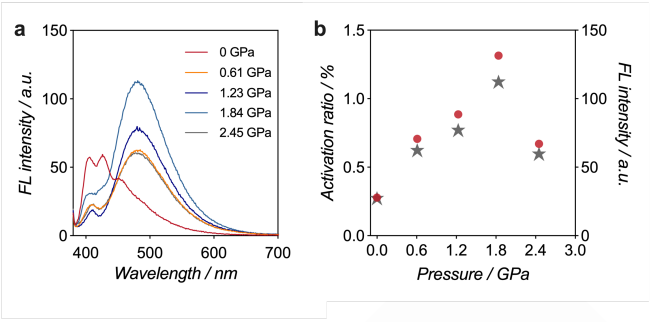

Figure 5. (a) Fluorescence spectra of molecules extracted from polymer **N*cis*** at different pressures (For 0 GPa, the peaks generation is due to slight residual of photo-initiator and swelling-induced release of **2**). (b) Plot of mechanophore activation ratio and fluorescence intensity I_{483} versus compression pressures. Red small dots represent the activation ratio, and the pentagrams represent fluorescence intensity.

We then sought to explore the release of our new fluorophore ATM in the solid state. Rotaxanes **1R-*cis/trans*** were modified into crosslinker **1X-*cis/trans*** by substituting the bromine for an azide group and subsequent click reaction with propargyl acrylate (Figure 1c, SI Section 3.3). These crosslinker rotaxanes (0.053 mol%) were combined with ethylene glycol dimethacrylate (0.947 mol%) and methyl acrylate to form PMA networks **N*cis*** and **N*trans*** (1 mol% total crosslinker density). These networks were obtained by photopolymerization, initiated from 2-hydroxy-2-methylpropiophenone (HMP) and UV light (365 nm), in rectangular mould (30×10×1.5 mm^3). The material was divided into equal portions (4×4×1.5 mm^3) and subjected to varying compression forces (0-2.45 GPa) with a manual press. The networks were swollen in acetonitrile after each compression to extract the released molecules. The presence of the ATM fluorophore in the extract was confirmed by ^{1}H NMR spectroscopy (Figure S22), and the release efficiency was quantified by fluorescence spectroscopy (Figures 5, S21). The concentration of ATM in the extract was determined by comparing the fluorescence intensity at 483 nm to a calibration curve (Figure S20). The release efficiency increases linearly with the compression force, peaking at 1.3% at 1.8 GPa before decreasing at higher compression level. The latter effect is attributed to an increasing rate of scission in the PMA backbone.[1a] As a result, the crosslinked poly(methyl acrylate) material with a specific crosslinking density (1 mol%) and mechanophore content (0.53‰ compared to MA monomer) achieved a maximum release amount of approximately 1.3%, which is comparable to the release ratio reported for a "flex-activated" anthracene-maleimide mechanophore.[7c]

In conclusion, we have described a mechanochromic rotaxane actuator that can release azetidine-trityl-maleimide, a new rigidochromic fluorescent dye with excellent chemical stability and optical properties. The release was demonstrated in solution and in a crosslinked network, and we found that the release efficiency was dependent on the relative position of the azetidine ring (either *cis* or *trans* to the rotaxane axle), with the *cis* isomer being the most reactive. The rotaxane actuation also proved to be more selective as the corresponding non-interlocked adduct is predicted to break at the C-N bond upon elongation. This demonstrates the unique ability of rotaxane actuator to elicit useful mechanochemical processes, such as the release of fluorescent probes. We envisage that such system could be used to read the stress history of a material, particularly if deployed in a multicargo system[9] that can release several ATM at the same location over multiple rounds of activation. The unique optical properties and the universal nature (chemical stability, polarity insensitive) of ATM also make this new dye an attractive probe for biological applications.

Acknowledgements

We thank the Engineering and Physical Sciences Research Council (EPSRC; grants no. EP/X023788/1 and EP/Y021282/1), Marie Skłodowska-Curie Individual Fellowships (to M. W., selected by MSCA, funded by EPSRC), and the European Research Council (ERC Consolidator selected by the ERC, funded by EPSRC) for funding. Additionally, we thank Reece Lister-Roberts, Dr Meera Mehta, and Dr George Whitehead for assistance with X-ray crystallographic analysis, and Dr Alexander Romanov for assistance with solid fluorescence quantum yield measurements.

Keywords: controlled release • fluorescent probes • maleimide • mechanophore • rotaxanes

10.1002/anie.202501499

[1] a) Y. Chen, G. Mellot, D. van Luijk, C. Creton, R. P. Sijbesma, *Chem. Soc. Rev.* **2021**, *50*, 4100; b) E. M. Lloyd, J. R. Vakil, Y. Yao, N. R. Sottos, S. L. Craig, *J. Am. Chem. Soc.* **2023**, *145*, 751.

[2] a) D. A. Davis, A. Hamilton, J. Yang, L. D. Cremar, D. V. Gough, S. L. Potisek, M. T. Ong, P. V. Braun, T. J. Martínez, S. R. White, J. S. Moore, N. R. Sottos, *Nature* **2009**, *459*, 68; b) M. J. Robb, T. A. Kim, A. J. Halmes, S. R. White, N. R. Sottos, J. S. Moore, *J. Am. Chem. Soc.* **2016**, *138*, 12328; c) M. Li, H. Zhang, F. Gao, Z. Tang, D. Zeng, Y. Pan, P. Su, Y. Ruan, Y. Xu, W. Weng, *Polym. Chem.* **2019**, *14*, 409; d) M. E. McFadden, M. J. Robb, *J. Am. Chem. Soc.* **2019**, *141*, 11388; e) T. Wang, H. Wang, L. Shen, N. Zhang, *Chem. Commun*. **2021**, *57*, 12675; f) H. Qian, N. S. Purwanto, D. G. Ivanoff, A. J. Halmes, N. R. Sottos, J. S. Moore, *Chem* **2021**, *7*, 1080; g) Y. Sagara, H. Traeger, J. Li, Y. Okado, S. Schrettl, N. Tamaoki, C. Weder, *J. Am. Chem. Soc.* **2021**, *143*, 5519; h) M. Wu, Y. Li, W. Yuan, G. De Bo, Y. Cao, Y. Chen, *J. Am. Chem. Soc.* **2022**, *144*, 17120; i) G. A. Filonenko, J. A. M. Lugger, C. Liu, E. P. A. van Heeswijk, M. M. R. M. Hendrix, M. Weber, C. Müller, E. J. M. Hensen, R. P. Sijbesma, E. A. Pidko, *Angew. Chem. Int. Ed.* **2018**, *57*, 16385.

[3] a) Y. Sagara, M. Karman, E. Verde-Sesto, K. Matsuo, Y. Kim, N. Tamaoki, C. Weder, *J. Am. Chem. Soc.* **2018**, *140*, 1584; b) Y. Sagara, M. Karman, A. Seki, M. Pannipara, N. Tamaoki, C. Weder, *ACS Cent. Sci.* **2019**, *5*, 874; c) T. Muramatsu, Y. Okado, H. Traeger, S. Schrettl, N. Tamaoki, C. Weder, Y. Sagara, *J. Am. Chem. Soc.* **2021**, *143*, 9884; d) R. S. Torrientes, T. Carr, G. De Bo, *Macromol. Rapid Comm.* **2021**, *42*, 2000447.

[4] a) Y. Chen, A. J. H. Spiering, S. Karthikeyan, G. W. M. Peters, E. W. Meijer, R. P. Sijbesma, *Nat. Chem.* **2012**, *4*, 559; b) K. Imato, A. Irie, T. Kosuge, T. Ohishi, M. Nishihara, A. Takahara, H. Otsuka, *Angew. Chem. Int. Ed.* **2015**, *54*, 6168; c) R. Göstl, R. P. Sijbesma, *Chem. Sci.* **2016**, *7*, 370; d) F. Verstraeten, R. Göstl, R. P. Sijbesma, *Chem. Commun.* **2016**, *52*, 8608; e) T. Sumi, R. Goseki, H. Otsuka, *Chem. Commun.* **2017**, *53,* 11885; f) H. Sakai, T. Sumi, D. Aoki, R. Goseki, H. Otsuka, *ACS Macro Lett.* **2018**, 7, 1359; g) K. Ishizuki, D. Aoki, R. Goseki, H. Otsuka, *ACS Macro Lett.* **2018**, *7*, 556; h) M. Karman, E. Verde-Sesto, C. Weder, *ACS Macro Lett.* **2018**, 7, 1028; i) M. E. McFadden, M. J. Robb, *J. Am. Chem. Soc.* **2021**, *143*, 7925; j) J. R. Hemmer, C. Rader, B. D. Wilts, C. Weder, J. A. Berrocal, *J. Am. Chem. Soc.* **2021**, *143*, 18859; k) H. Sugita, Y. Lu, D. Aoki, H. Otsuka, K. Mikami, *Chem. A Eur. J.* **2023**, *29*, e202203249.

[5] a) M. Karman, E. Verde-Sesto, C. Weder, Y. C. Simon, *ACS Macro Lett.* **2018**, *7*, 1099; b) M. Tan, Z. Hu, Y. Dai, Y. Peng, Y. Zhou, Y. Shi, Y. Li, Y. Chen, *ACS Macro Lett.* **2021**, *10*, 1423; c) X. Wang, Y. Cao, Y. Peng, L. Wang, W. Hou, Y. Zhou, Y. Shi, H. Huang, Y. Chen, Y. Li, *ACS Macro Lett.* **2022**, *11*, 310; d) M. Tan, X. Wang, T. Xie, Z. Zhang, Y. Shi, Y. Li, Y. Chen, *Macromolecules* **2022**, *55*, 6860.

[6] S. He, M. Stratigaki, S. P. Centeno, A. Dreuw, R. Göstl, *Chem. A Eur. J.* **2021**, *27*, 15889.

[7] a) X. Hu, T. Zeng, C. C. Husic, M. J. Robb, *J. Am. Chem. Soc.* **2019**, *141*, 15018; b) Z. Shi, Q. Song, R. Göstl, A. Herrmann, *CCS Chem.* **2021**, *3*, 2333; c) F. Yang, T. Geng, H. Shen, Y. Kou, G. Xiao, B. Zou, Y. Chen, *Angew. Chem. Int. Ed.* **2023**, *62*, e202308662; d) Y.-L. Tseng, T. Zeng, M. J. Robb, *Chem. Sci.* **2024**, *15*, 1472; e) P. Liu, Y.-L. Tseng, L. Ge, T. Zeng, D. Shabat, M. J. Robb, *J. Am. Chem. Soc.* **2024**, *146*, 22151.

[8] T. Zeng, L. A. Ordner, P. Liu, M. J. Robb, *J. Am. Chem. Soc.* **2024**, *146*, 95.

[9] L. Chen, R. Nixon, G. De Bo, *Nature* **2024**, *628*, 320.

[10] a) R. Klajn, *Chem. Soc. Rev*. **2014**, *43*, 148; b) X. Qin, X. Yang, L. Du, M. Li, *RSC Med. Chem*. **2021**, *12*, 1826; c) A. L. D. Wallabregue, H. Bolland, S. Faulkner, E. M. Hammond, S. J. Conway, *J. Am. Chem. Soc*. **2023**, *145*, 2572; d) Y. Shi, F. Huo, C. Yin, *Analyst*, **2023**, *148*, 3491; e) P. Kumar, R. Kaushilk, D. A. Jose, *Anal. Chem*. **2016**, *88*, 11314.

[11] J. Barker, J. Tibbetts, C. Ferguson, Y. Xie, R. K. O'Reilly, *Angew. Chem. Int. Ed.* **2024**, *63*, e202410550.

[12] a) A. B. Mabire, M. P. Robin, W.-D. Quan, H. Willcock, V. G. Stavros, R. K. O'Reilly, *Chem. Commun.* **2015**, *51*, 9733; b) M. Staniforth, W.-D. Quan, T. N. V. Karsili, L. A. Baker, R. K. O'Reilly, V. G. Stavros, *J. Phys. Chem. A* **2017**, *121*, 6357; c) Y. Xie, J. T. Husband, M. Torrent-Sucarrat, H. Yang, W. Liu, R. K. O'Reilly, *Chem. Commun.* **2018**, *54*, 3339.

[13] J. T. Husband, Y. Xie, T. R. Wilks, L. Male, M. Torrent-Sucarrat, V. G. Stavros, R. K. O'Reilly, *Chem. Sci.* **2021**, *12*, 10550.

[14] W. Chi, P.-P. Sun, *Phys. Chem. Chem. Phys.* **2023**, *25*, 4193.

[15] J. Ormson, A. Duwez, G. De Bo in *Mechanically Interlocked Materials*, *Chapter 1* (Eds.: E. M. Pérez), Wiley, **2024**, pp. 1–28.

[16] G. E. Sanoja, X. P. Morelle, J. Comtet, C. J. Yeh, M. Ciccotti, C. Creton, *Sci. Adv.* **2021**, *7*, eabg9410.

[17] W. Xi, T. B. Saw, D. Delacour, C. T. Lim, *Nat. Rev. Mater.* **2019**, *4*, 23.

[18] L. Chen, G. De Bo, *J. Am. Chem. Soc.* **2024**, *146*, 16381.

[19] Deposition number 2415977 (for **8**$_{cis}$) contains the supplementary crystallographic data for this paper. These data are provided free of charge by the joint Cambridge Crystallographic Data Centre and Fachinformationszentrum Karlsruhe Access Structures service.

[20] A. Anastasaki, V. Nikolaou, G. Nurumbetov, P. Wilson, K. Kempe, J. F. Quinn, T. P. Davis, M. R. Whittaker, D. M. Haddleton, *Chem. Rev.* **2016**, *116*, 835.

[21] M. Beyer, *J. Chem. Phys.* **2000**, *112*, 7307.

[22] I. M. Klein, C. C. Husic, D. P. Kovács, N. J. Choquette, M. J. Robb, *J. Am. Chem. Soc.* **2020**, *142*, 16364.

[23] For recent examples see: a) Q. Cheng, G. De Bo, *Chem. Sci.* **2024**, *15*, 13181; b) D. Xu, W. Liu, S. Tian, H. Qian, *Angew. Chem. Int. Ed.* **2025**, 64, e202415353; c) M. Horst, J. Meisner, J. Yang, T. B. Kouznetsova, S. L. Craig, T. J. Martínez, Y. Xia, *J. Am. Chem. Soc.* **2024**, *146*, 884; d) S. Ding, W. Wang, A. Germann, Y. Wei, T. Du, J. Meisner, R. Zhu, Y. Liu, *J. Am. Chem. Soc.* **2024**, 146, 6104; e) K. Suwada, A. W. Ieong, H. L. H. Lo, G. De Bo, *J. Am. Chem. Soc.* **2023**, *145*, 20782.

10.1002/anie.202501499

WILEY VCH

COMMUNICATION

Entry for the Table of Contents

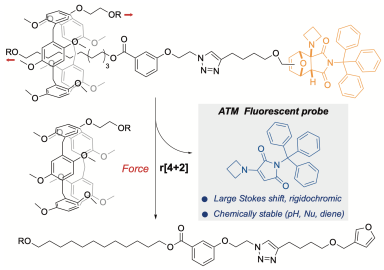

A mechanochromic rotaxane capable of releasing azetidine-trityl-maleimide (ATM), a new fluorescent probe displaying excellent optical properties (rigidochromic, large Stokes shift, solvent insensitive) and chemical stability (pH, nucleophiles, dienes), is presented. The mechanochemical generation of ATM is only possible with a rotaxane actuator, and this device should find applications in materials and biological science.

Institute and/or researcher Twitter usernames: @guillaumedebo, Bluesky: @guillaumedebo.bsky.social